

Contribution from the Department of Chemistry and Division of Engineering, Brown University, Providence, Rhode Island 02912, and the Department of Chemistry and Institute of Materials Science, University of Connecticut, Storrs, Connecticut 06268

Preparation and Properties of Iron Phosphorus Triselenide, FePSe₃^{1a}

B. TAYLOR, J. STEGER, A. WOLD,* and E. KOSTINER^{1b}

Received May 3, 1974

AIC40287N

Iron phosphorus triselenide, FePSe₃, has been prepared by chemical vapor transport using 75 Torr of chlorine gas as a transport agent and a temperature gradient of 650–>610°. The structure of FePSe₃ (space group R3) is related to that of CdI₂. Selenium atoms are in a hexagonal, close-packed array with iron atoms and phosphorus-phosphorus pairs (2:1 ratio) occupying the trigonally distorted octahedral holes in an ordered arrangement. Magnetic susceptibility measurements show that the compound orders antiferromagnetically at 123 (2)°K; Mossbauer effect measurements indicate the principal axis of magnetization is along the crystallographic (hexagonal) *c* axis. The paramagnetic moment and Mossbauer data obtained above the ordering temperature indicate that the iron ions exist in the divalent high-spin state.

Introduction

The preparation and crystal structure of compounds with the general formula MPX₃, where M = Mn, Fe, Co, Ni and X = S, Se, was first reported by Klingen, *et al.*²⁻⁵ Later work on the sulfides⁶ showed that these compounds exhibit antiferromagnetic ordering. However, there have been no reported studies of the corresponding selenide compounds.

The crystal structure of FePSe₃ has been determined by Klingen.⁵ The reported lattice parameters for the hexagonal unit cell (space group R3) are $a_0 = 6.27$ Å and $c_0 = 19.80$ Å; theoretical density 4.79 g/cm³; $Z = 6$. The structure is related to that of CdI₂, with iron atoms and phosphorus-phosphorus pairs occupying the cadmium positions and selenium atoms the iodine positions. This atomic arrangement results in FeSe₆ and P₂Se₆ octahedral groups. The P-P bond direction is collinear with the octahedral threefold axis and is parallel with the hexagonal *c* axis. The octahedral coordination about the iron atoms and the P-P pairs is shown in Figure 1 by the shaded circles.

Mossbauer effect data obtained in an earlier study of FePS₃⁷ were not definitive because this compound crystallizes in a lower symmetry monoclinic space group (but with essentially the same crystalline arrangement). The higher symmetry of the FePSe₃ space group allows an unambiguous interpretation of the Mossbauer data.

Experimental Section

1. Preparation. Single crystals of FePSe₃ were grown by chemical vapor transport. The proper weights of high-purity (99.99%) starting materials were placed in silica tubes, evacuated to 2×10^{-3} Torr, back-filled with 75 Torr of chlorine gas, and then sealed. The chemical vapor transport reactions were carried out in a two-zone furnace. Reverse transport was carried out for 24 hr to reduce the number of nucleating centers. The furnace was then equilibrated at 650° for 3–6 hr; the final temperature gradient (650–>610°) was obtained by the gradual cooling (1°/hr) of the growth zone.

2. X-Ray Analysis. Samples prepared by the above procedures were analyzed by fast scan (1° 2θ/min) X-ray diffractometry to en-

sure that the materials were single phase and then by slow scan (1/4° 2θ/min) to obtain precision lattice parameters (internal standard MgO). A Norelco diffractometer with monochromatic radiation and a high-intensity copper source was used [$\lambda(\text{Cu K}\alpha_1)$ 1.5405 Å]. Lattice parameters were obtained from a least-squares analysis of the data.

3. Density Measurements. Density measurements were made on single-crystal samples by a hydrostatic technique⁸ using perfluoro-1-methyldecalin as the liquid which was first calibrated using a crystal of high-purity silicon (density 2.328 g/cm³). All measurements were made at $25 \pm 2^\circ$.

4. Magnetic Measurements. Magnetic susceptibility measurements on ground single-crystal samples were carried out using a Faraday balance⁹ equipped with a Cahn RG electrobalance over the temperature range 77–500°K and at field strengths between 6.25 and 10.30 kOe.

5. Mossbauer Effect Measurements. The iron-57 Mossbauer spectra of FePSe₃ were measured with a Model NS-1 Mossbauer spectrometer (Nuclear Science and Engineering Corp.) operating in the constant-acceleration mode. The 14.4-keV γ radiation from a source of 20-mCi ⁵⁷Co diffused into Pd was detected with a gas proportional counter and collected with a 400-channel analyzer (Nuclear Chicago Corp.) operating in time-sequence scaling mode. The source and drive were calibrated against a single crystal of sodium iron(II) nitropentacyanide dihydrate. The quadrupole splitting of this standard was taken as 1.7048 mm/sec.¹⁰ Isomer shifts are reported with respect to the zero position of this standard. The data were computer fit with a maximum likelihood regression analysis program to a product of Lorentzian profiles superposed on a parabolic base line, a result of the drive geometry. All parameters—peak position, half-width and -height—were allowed to vary independently. Cryogenic measurements were made in a variable-temperature dewar (Andonian Associates, Inc.).

Results and Discussion

The X-ray diffraction results from four samples of ground single crystals indicate that FePSe₃ has rhombohedral symmetry. The average lattice parameters (hexagonal cell) are $a_0 = 6.262$ (3) Å and $c_0 = 19.810$ (6) Å with a calculated density of 4.794 (3) g/cm³ and an average measured density of 4.77 (1) g/cm³. These values are in good agreement with those previously reported.⁵ Table I gives the values of *hkl* and the observed and calculated values of $\sin^2 \theta$ for the indexed powder pattern of FePSe₃.

Magnetic susceptibility data were collected for three samples of FePSe₃ over the temperature range 77–500°K. A typical plot of $1/\chi_M$ vs. *T* (Figure 2) indicates that the material orders antiferromagnetically at 123 (2)°K. Honda–Owen plots¹¹ of all samples were made to determine the presence of any ferromagnetic impurities; none were detected in any of the samples.

(8) L. J. Cabri, *Amer. Mineral.*, **54**, 539 (1969).

(9) B. Morris and A. Wold, *Rev. Sci. Instrum.*, **39**, 1937 (1968).

(10) R. W. Grant, R. M. Housley, and U. Gonser, *Phys. Rev.*, **178**, 523 (1969).

(11) K. Honda, *Ann. Phys. (Leipzig)*, **32** (337), 1048 (1910); M. Owen, *ibid.*, **37** (342), 657 (1912).

* To whom correspondence should be addressed at Brown University.

(1) (a) This research has been supported by NSF Grant No. GH-37104 and GH-33631. Acknowledgment is also made to Brown University's Materials Sciences Laboratory, funded through the National Science Foundation—GH-33631. (b) This author's contribution was supported by the University of Connecticut Research Foundation.

(2) H. Hahn and W. Klingen, *Naturwissenschaften*, **52**, 494 (1965).

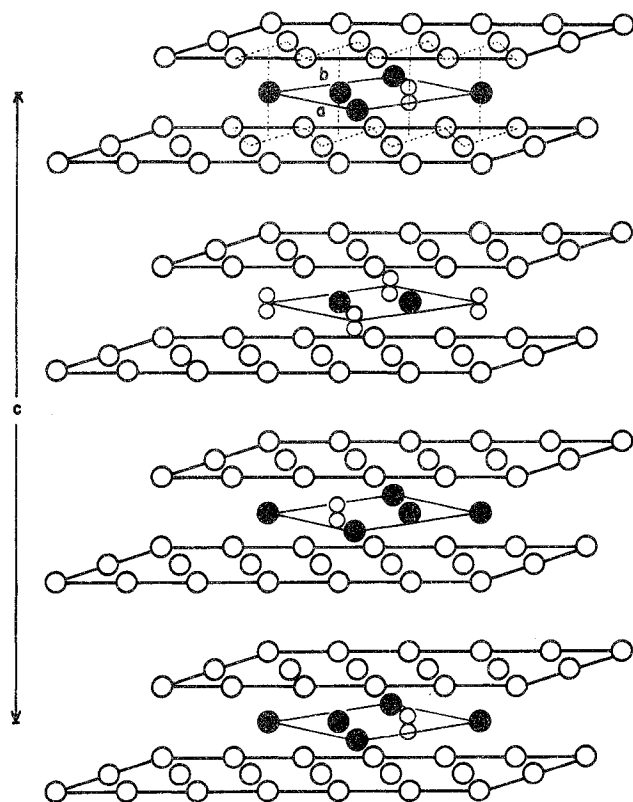
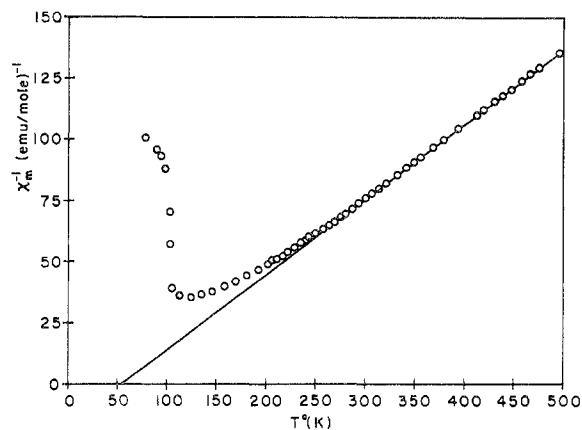
(3) (a) W. Klingen, G. Eulenberger, and H. Hahn, *Naturwissenschaften*, **55**, 229 (1968); (b) *ibid.*, **57**, 88 (1970).

(4) W. Klingen, G. Eulenberger, and H. Hahn, paper presented at the Meeting on Transition Metal Compounds, Oslo, Norway, 1969.

(5) W. Klingen, Thesis, Universität Hohenheim, 1969.

(6) R. Nitsche and P. Wild, *Mater. Res. Bull.*, **5**, 419 (1970).

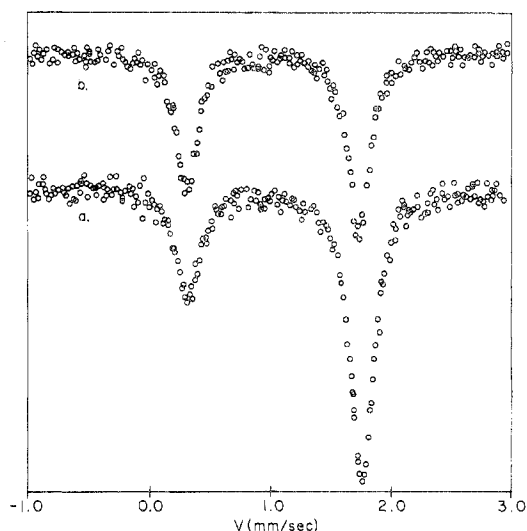
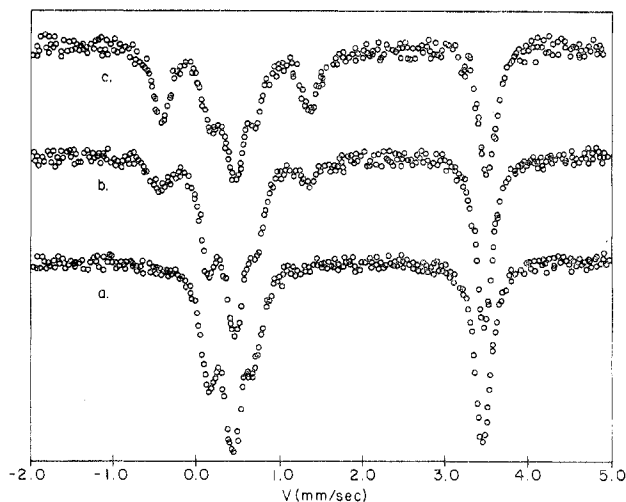
(7) B. Taylor, J. Steger, and A. Wold, to be submitted for publication in *J. Solid State Chem.*

Figure 1. Schematic structure of FePSe_3 .Figure 2. Graph of $1/X_M$ vs. T for a ground crystal of FePSe_3 .Table 1. Powder Indexing for FePSe_3 ,^a

<i>hkl</i>	$\sin^2 \theta$		<i>hkl</i>	$\sin^2 \theta$	
	Obsd	Calcd		Obsd	Calcd
113	0.07414	0.07414	226	0.29639	0.29658
116	0.11497	0.11499	0,0,15	0.34044	0.34041
009	0.12236	0.12255	413	0.43733	0.43732
119	0.18284	0.18308	0,0,18	0.48996	0.49019
306	0.23608	0.23605	1,1,18	0.55062	0.55072
223	0.25599	0.25573	1,1,21	0.72793	0.72773
1,1,12	0.27854	0.27839			

^a Only reflections used in precision lattice parameter calculations are shown.

The effective magnetic moment ($P_{\text{eff}} = 5.08(5)$ BM) determined from a least-squares fit of the data in the paramagnetic region indicates that iron is present in a high-spin divalent state. Extrapolation of the inverse paramagnetic susceptibility data to zero results in a positive Weiss constant ($\Theta = 37(2)^\circ\text{K}$).

Figure 3. Room-temperature (296°K) Mossbauer spectra for an FePSe_3 single crystal as a function of the angle (θ) between the c crystallographic axis and the incident γ direction: a, $\theta = 0^\circ$; b, $\theta = 45^\circ$.Figure 4. Liquid nitrogen temperature (77°K) Mossbauer spectra for an FePSe_3 single crystal as a function of the angle (θ) between the c crystallographic axis and the incident γ direction: a, $\theta = 0^\circ$; b, $\theta = 22.5^\circ$; c, $\theta = 45^\circ$.

Room-temperature Mossbauer spectra of FePSe_3 (Figure 3) were obtained for two different orientations of a single-crystal sample. The crystal was first mounted with the hexagonal c axis parallel to the incident γ radiation (the orientation was verified using the back-reflection Laue technique) and then reoriented so that the angle between the incident γ radiation and the c axis was 45° .

For the case when the Mossbauer electric field gradient asymmetry parameter (η) is zero the general expressions for the relative intensities of a quadrupole-split absorption are given by eq 1 and 2,¹² where θ is the angle between the direc-

$$I_1 = 1 + \frac{3}{2} \sin^2 \theta \quad (1)$$

$$I_2 = \frac{3}{2} (1 + \cos^2 \theta) \quad (2)$$

tion of the γ radiation and the unique crystallographic axis.

Since FePSe_3 has a rhombohedral structure with cations

Table II. Mossbauer Effect Parameters for FePSe₃

$\theta, ^\circ$ deg	$T, ^\circ$ K	IS, ^b mm/sec	$\Delta E_Q, \text{mm/sec}$	H, kOe	I	I values		$e^2qQ/2, \text{mm/sec}$
						Obsd	Calcd	
0	296 (1)	1.05 (1)	1.449 (5)		I_1/I_2	0.37 (2)	0.333	
45	296 (1)	1.06 (1)	1.441 (5)		I_1/I_2	0.77 (2)	0.778	
0	77 (1)				$I_2 + I_4$	0.35 (2)	0.333	
					$I_3 + I_6$			
22.5	77 (1)	1.19 (2)		95 (2)	$I_1 + I_5$	0.12 (2)	0.105	1.53 (1)
					$I_3 + I_6$			
					$I_2 + I_4$	0.37 (2)	0.333	
					$I_3 + I_6$			
45	77 (1)	1.20 (2)		96 (2)	$I_1 + I_5$	0.48 (2)	0.444	1.52 (1)
					$I_3 + I_6$			
					$I_2 + I_4$	0.32 (2)	0.333	
					$I_3 + I_6$			

^a θ is the angle between incident γ direction and the c crystallographic axis. ^b Isomer shifts are with respect to the 0 position of sodium iron(II) nitropentacyanide dihydrate.

on threefold axes, the observed intensities of the quadrupole-split pair should follow eq 1 and 2. The excellent agreement between the observed and calculated intensity ratios for $\theta = 0$ and 45° can be seen in Table II. The isomer shift and quadrupole splitting are characteristic of high-spin Fe d⁶ in an octahedral environment. Furthermore, the energies of the quadrupole-split lines ($E_{I_1} < E_{I_2}$) indicate that the electric field gradient tensor is positive.

In agreement with the bulk antiferromagnetism observed in the magnetic susceptibility measurements, the Mossbauer spectrum of FePSe₃ taken at 77°K shows the presence of a magnetic hyperfine interaction (see Figure 4). The intensity equations for the hyperfine spectrum are¹²

$$I_1 = I_5 = \frac{4}{3} \sin^2 \theta \quad (3)$$

$$I_2 = I_4 = \frac{1}{3} (1 + \cos^2 \theta) \quad (4)$$

$$I_3 = I_6 = 1 + \cos^2 \theta \quad (5)$$

where θ is the angle between the principal axis of magnetization and the incident γ radiation.

In order to determine the correct assignment of the energy level diagram and to demonstrate that the principal axis of magnetization is parallel to the hexagonal c axis, data were collected at 77°K for three orientations of single-crystal FePSe₃. As shown in Figure 4, the (I_1, I_5) hyperfine transitions are absent with $\gamma \parallel c$ but are apparent when γ is at an

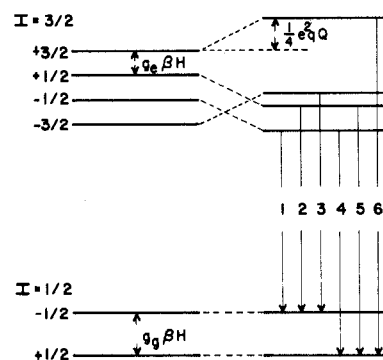


Figure 5. Schematic energy level diagram for ⁵⁷Fe in FePSe₃ below the Neel point with $\eta = 0, H \parallel V_{zz}, e^2qQ > 0$, and $|5g_e\beta_n H| = |e^2qQ|$.

angle of 22.5° to c and are even more intense when γ and c form an angle of 45° . The relative intensities calculated from eq 3-5 and the observed relative intensities at 0, 22.5, and 45° are in good agreement and are given in Table II. These results show clearly that the principal axis of magnetization is parallel (within experimental error) to the hexagonal c axis.

The energy level diagram determined from the positions of the various hyperfine transitions is shown in Figure 5; the internal magnetic field has a calculated value of 95 (2) kOe at 77°K.

Registry No. FePSe₃, 52226-00-3.